shield, respectively. In the other prototype, a pair of single conductor 30 AWG wires were epoxied at diametrically opposed points in the jacket and shield to form resistor circuits. Comparative absorbed dose rate measurements were performed at a depth of 2.5 cm in a water-equivalent phantom, under otherwise standard conditions, in a 6 MV photon beam. The stability of the thermal control, as well as the magnitude and repeatability of the calorimeter responses were evaluated.

Results

For both prototypes, the core power dissipation exhibited a typical level of stability on the order of 1.5 μW/min, with an associated 1σ signal variation of 1.2 μW, or equivalently, an absorbed dose rate variation of about 0.1 Gy/min. In terms of thermal stability, the core temperature was maintained to within about 10 μK (1σ) under both control systems once adequately tuned.

Under irradiation, the thermistor-heated and graphite-heated GPC recorded an absorbed dose rate to graphite of 5.05 ± 0.04 Gy/min and 5.10 ± 0.04 Gy/min, with an associated repeatability (1σ) of 0.4 % and 0.5 %, respectively.

Conclusion

This work demonstrates the feasibility of resistive dissipation directly in the GPC's graphite as a practical means of achieving thermal control, as no significant differences were observed in the two constructed prototypes under irradiation. The practical impact of adopting in-graphite heating is a considerable reduction in the overall manufacturing cost, both in terms of materials and complexity of the assembly, and may be of benefit to national metrology institutes for their future designs.

OC-0078 A formalism for the assessment of dosimetric uncertainties due to positioning uncertainties

W. Lechner[1], D. Georg[1], H. Palmans[2]
[1]*Medizinische Universität Wien, Department of Radiotherapy and Christian Doppler Laboratory for Medical Radiation Research for Radiation Oncology, Vienna, Austria*
[2]*National Physical Laboratory, Radiation Dosimetry, Teddington, United Kingdom*

Purpose or Objective

The assessment of the type-B uncertainty due to detector positioning in small photon fields. This uncertainty can be caused by uncertainties in the determination of the position of the maximum dose, the step width of the scanning phantom and uncertainties in collimator (re-)positioning when changing the field size. While positioning makes up an important contribution to the overall dosimetric uncertainty of small fields, there is limited consensus how to assess this uncertainty and published uncertainty estimates for similar experimental conditions can vary by up to an order of magnitude.

Material and Methods

Assuming that the beam profile of small photon fields near the maximum dose can be approximated by a second order polynomial (D(x)) and the probability distribution of the relative position of the detector (x) to the position of the maximum dose (x0) within a maximum displacement (a) can be described by a rectangular function (p(x)), the expectance value (E), its variance (var) and relative type-B standard uncertainty, u_{B,r}, can be expressed as:

$$D(x) = p_0 + p_1 x + p_2 x^2 \quad (1)$$

$$p(x) = \frac{1}{2a} \quad (2)$$

$$E = \int_{-a}^{a} D(x + x_0) p(x) dx = p_0 - \frac{{p_1}^2}{4p_2} + \frac{a^2 p_2}{3} \quad (3)$$

$$var = \sigma^2 = \int_{-a}^{a} (D(x + x_0) - E)^2 p(x) dx = \frac{4a^4 {p_2}^2}{45} \quad (4)$$

$$u_{B,r} = \frac{\sqrt{\sigma^2}}{E} \quad (5)$$

A beam profile of a 0.5 x 0.5 cm² 6 MV beam produced by a Versa HD (Elekta AB, Stockholm, Sweden) was acquired using a microDiamond (PTW, Freiburg, Germany) with a step width of 0.1 mm. Eq. (1) was fitted to the measured beam profile. The relative standard uncertainty contribution to the absorbed dose, u_{B,r} was calculated according to Eq. (5) and plotted as a function of the maximum deviation (a) between detector and maximum dose in Fig. 1.

Results

As expected, the relative standard uncertainty contribution to the absorbed dose due to uncertainties in detector positioning increased with increasing maximum detector displacement relative to the maximum dose. For a maximum displacement of 0.2 mm, 0.5 mm and 1 mm the uncertainty was below 0.1%, 0.5% and 1.9%, respectively.

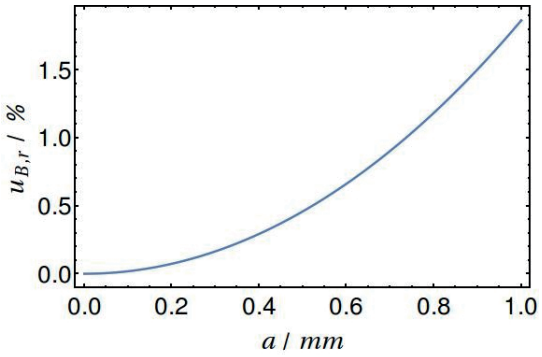

Figure 1: standard uncertainty as a function of maximum deviation between the detector position and the maximum dose.

Conclusion

The proposed formalism allows an assessment of the relative standard uncertainty contribution to the absorbed dose due to positioning uncertainties based on beam profile measurements and could contribute to harmonization of uncertainty estimation in small field dosimetry. The example given, which is representative for typical small fields of size 0.5 cm, shows that positioning tolerance in dosimetry should be below 0.5 mm for limiting the uncertainty contribution to 0.5%.

OC-0079 A new multi-purpose QA phantom for use on the Elekta MR-Linac

I. Hanson[1], J. Sullivan[1], S. Nill[1], U. Oelfke[1]
[1]*The Institute of Cancer Research and The Royal Marsden NHS Foundation Trust, Joint Department of Physics, Sutton, United Kingdom*

Purpose or Objective

Performing routine quality assurance (QA) measurements on an MR Linac is complicated by several factors. Amongst these are the presence of a magnetic field, the lack of a light field, the fixed angle of the collimating system and the inaccessibility of the treatment head.

A new phantom has been developed to address these issues. The phantom makes use of the fixed EPID panel present on the Elekta MR-Linac (Elekta Unity, Elekta AB,

Stockholm, Sweden) to check for absolute gantry angle, jaw and leaf bank alignment, EPID panel rotation, EPID offset, EPID scaling and the alignment of the MR imaging and the MV isocenter.

Material and Methods

The phantom consists of two main components, a plumb-line and a water-level. Initially separated prototypes of these systems are shown in figure 1.

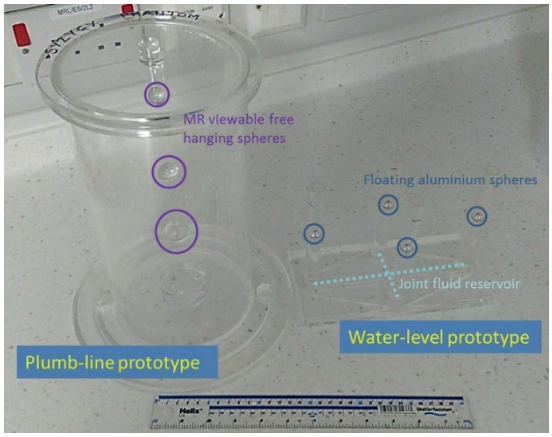

The plumb-line component consists of 3 free-hanging spheres filled with an MR observable liquid. An EPID image acquired at gantry angle zero (GA0) will only show concentric circles when the phantom is correctly lined up at the isocentre and the linac is at true vertical. This image will also test the position of the fixed EPID, as the reference point of the EPID (the isocentre-pixel) will be at the centre of concentric circles.

The water-level phantom component consists of 4 aluminium spheres floating in water from a joint reservoir. An EPID image acquired of this phantom will show concentric circles only when the height of the spheres are at the linac isocentre height and the GA of the linac is at 90 or 270 degrees. As above, the centre of these concentric spheres will correspond to the isocentre pixel of the fixed EPID.

Imaging the plumb-line (vertical) and water-level (horizontal) will test the fixed rotation angle of the radiation collimation system along with the EPID rotation angle. Known distances between spheres will furthermore test the correct distance scaling of the EPID panel.

Finally the plumb-line spheres can be imaged with the MR scanner. Relating the coordinates of the MR image to the EPID coordinates will test the alignment between the MR and the MV radiation isocentre.**Results**

Figure 2 shows edge-enhanced EPID images acquired of the plumb-line prototype at a gantry angles of 0, 1 and 0.2 degrees, and the water-level prototype at gantry angles of 90, 91 and 90.2 degrees. As can be seen there is a clear offset in the overlap of the spheres in the EPID images when not acquired perfectly at GA0 or GA90

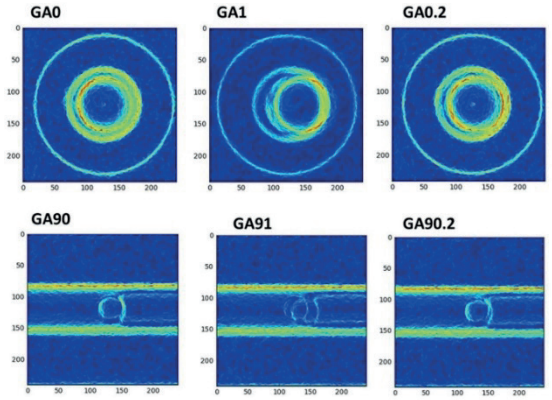

Table 1 shows that good agreement was found between the MR to MV alignment values found with the plumb-line and the official Elekta phantom

MR to MV alignment (mm)	L/R	S/I	A/P
Plumb line	+0.93	-1.43	+0.5
Elekta phantom	+0.79	-1.09	+0.44

Conclusion

The prototype components of a new MR-Linac QA phantom have been developed and tested. It has been demonstrated that they provide a good check of gantry angle, EPID position and MR to MV alignment. The main strength of this phantom is that these measurements are solely dependent on an absolute metric, gravity, rather than any phantom or linac manufacturing tolerances.

OC-0080 Dosimetric evaluation of a 3D printed phantom for patient-specific pre-treatment plan verification

D.N. Makris[1], E. Zoros[2], T. Boursianis[3], E. Pappas[4], T.G. Maris[3], E.P. Efstathopoulos[1]

[1]*Medical School-National and Kapodistrian University of Athens, Second Department of Radiology, Athens, Greece*
[2]*Medical School-National and Kapodistrian University of Athens, Medical Physics Laboratory, Athens, Greece*
[3]*University of Crete- Heraklion- Crete- Greece, Department of Medical Physics, Heraklion, Greece*
[4]*Technological Educational Institute of Athens- Greece, Department of Radiology and Radiotherapy, Athens, Greece*

Purpose or Objective

Stereotactic radiosurgery (SRS) is a well-established treatment approach for the management of a wide variety of lesions, mainly in the brain. Patient-specific dose verification becomes paramount in SRS treatments where small photon beams and steep dose gradients are employed. Although current patient-specific quality assurance techniques could detect critical dose errors, the dose distribution is not directly measured but is instead reconstructed. The scope of this work is to study the dosimetric characteristics of a 3D printed phantom based on anonymized real patient's CT scan and pave the way towards a truly patient-specific plan verification methodology.

Material and Methods

Using the treatment planning CT scan of a real patient with 6 brain metastases (target volumes of 0.023 - 0.989cc), a 3D model of the patient's external contour and bone structures was constructed. Patient skin was modelled by applying a 3mm thickness to the external contour. The model was cropped till the lower jaw, while patient immobilization apparatus was removed. A commercially available 3D printer was selected for 3D printing of the model, based on studied radiologic characteristics of the 3D-printed material samples. The hollow 3D-printed phantom was filled with polymer gel (tissue equivalent) and CT scanned using the same immobilization apparatus. In order to dosimetrically evaluate the phantom, the real patient's treatment plan was applied to the phantom's CT scan and corresponding calculated 3D dose distribution was exported. Following an anatomic based co-registration of the two CT scans, patient and phantom dose distributions were compared in terms of 1D profiles, 2D isolines, 3D gamma index (passing criteria: 1%/1mm), target and critical organs Dose Volume Histograms (DVHs) and plan quality metrics.

Results

The 3D printed material is bone equivalent in terms of HU (mean HU = 1037±57) which also applies to the printed "skin". All 1D profiles evaluated showed very good agreement in both soft tissue and bone structures, while a mean discrepancy of up to 8% was observed for the skin dose, as expected. An additional dose offset was